

## Original Article

# In vitro bioactivity of newly introduced dual-cured resin-modified calcium silicate cement

Ahmed Elbanna<sup>1</sup>, Dina Atta<sup>2</sup>, Dalia I. Sherief<sup>1</sup>

<sup>1</sup>Department of Biomaterials, Faculty of Dentistry, Ain-Shams University, <sup>2</sup>Department of Spectroscopy, Physics Division, National Research Centre, Cairo, Egypt

## ABSTRACT

**Background:** This study was designed to investigate the *in vitro* bioactivity of a new dual cured calcium silicate cement (TheraCal PT) compared to its light cured (TheraCal LC) and chemically set (Biodentine) counterparts.

**Materials and Methods:** The study is an *in vitro* original research article. Prepared cements discs were immersed in deionized water. Ca<sup>2+</sup> release was evaluated using inductively coupled plasma-optical emission spectrometry while pH was assessed using a pH meter after 1, 14, and 28 days. Discs for surface characterization were immersed in phosphate-buffered saline (PBS) and were examined using an environmental scanning electron microscope with energy dispersive X-ray (ESEM/EDX), immediately after setting and at 1, 14, and 28 days intervals after that. Attenuated total reflectance (ATR)/Fourier transform infrared (FTIR) and Raman spectroscopy analyses were performed after setting and after 28 days storage in PBS. Statistical analysis was performed using the two-way repeated measure analysis of variance test followed by Bonferroni test for multiple comparisons ( $P < 0.05$ ).

**Results:** Biodentine exhibited the highest mean values for Ca<sup>2+</sup> release (792,639,278 ppm) and pH (10.99, 12.7, 11.54) at all time intervals. ESEM/EDX displayed a continuous layer of calcium phosphate formed by Biodentine and TheraCal LC while TheraCal PT developed scarce interrupted precipitates after immersion in PBS. ATR/FTIR and Raman spectroscopy for the formed precipitates confirmed the presence of phosphate and Ca (OH)<sub>2</sub> in Biodentine, TheraCal LC and TheraCal PT.

**Conclusion:** TheraCal PT exhibited limited *in vitro* bioactivity which may limit its prognosis in clinical applications for vital pulp therapy. TheraCal LC is considered a potential bioactive calcium silicate cement despite its lower Ca<sup>2+</sup> release compared to Biodentine. Highest bioactivity was observed in Biodentine.

**Key Words:** Calcium silicate, dental cements, dental pulp capping, hydrogen ion concentration, pulpotomy

Received: 17-Feb-2021  
Revised: 21-Jun-2021  
Accepted: 23-Jul-2021  
Published: 28-Jan-2022

### Address for correspondence:

Dr. Ahmed Elbanna,  
Department of  
Biomaterials, Faculty of  
Dentistry, Ain-Shams  
University, Cairo, Egypt.  
E-mail: doctorbanna@asfd.  
asu.edu.eg

## INTRODUCTION

Bioactive materials are utilized in pulpal and further endodontic procedures to promote healing and

minimize the potential for extraction. Tricalcium and dicalcium silicates, the main phases present in commercial portland cements, tend to exhibit such

This is an open access journal, and articles are distributed under the terms of the Creative Commons Attribution-NonCommercial-ShareAlike 4.0 License, which allows others to remix, tweak, and build upon the work non-commercially, as long as appropriate credit is given and the new creations are licensed under the identical terms.

**For reprints contact:** WKHLRPMedknow\_reprints@wolterskluwer.com

**How to cite this article:** Elbanna A, Atta D, Sherief DI. *In vitro* bioactivity of newly introduced dual-cured resin-modified calcium silicate cement. Dent Res J 2022;19:1.

### Access this article online



Website: [www.drj.ir](http://www.drj.ir)  
[www.drjjournal.net](http://www.drjjournal.net)  
[www.ncbi.nlm.nih.gov/pmc/journals/1480](http://www.ncbi.nlm.nih.gov/pmc/journals/1480)

bioactivity. Their action is attributed to their capability to release  $\text{Ca}^{2+}$  and initiate apatite crystals precipitation when exposed to phosphate-containing physiological fluids. Mineral trioxide aggregate (MTA), a portland cement-based material, emerged in the early 1990's as a root-end filling material owing to its hydraulic properties and sealing ability.<sup>[1,2]</sup>

The term hydraulic calcium silicate cement (HCSC) is used to address the entire family of MTA-like cements.<sup>[1]</sup> The powder of HCSCs is formed chiefly of dicalcium and tricalcium silicates whose reaction together yields a sticky colloidal calcium silicate hydrate gel that finally solidifies into a hard structure.<sup>[3]</sup> HCSCs are frequently used in endodontic techniques including pulp capping, pulpotomy, apexogenesis, apexification, perforation repair, and root-end filling thanks to their biocompatibility as well as their setting and sealing ability in moist bloody fields.<sup>[4-6]</sup>

Various HCSCs have since emerged to overcome drawbacks of the original MTA cements such as long setting time, difficult handling, solubility and limited radiopacity.<sup>[7]</sup> Among such HCSCs is Biodentine™ (Septodont) which was formulated as a dentine replacement material.<sup>[8]</sup> The physical properties of Biodentine were modified via the alteration of powder composition, inclusion of setting accelerators and softeners together with using a predosed capsule configuration to be mixed in a triturator, making its handling more convenient.<sup>[9,10]</sup>

Biodentine hydrates in the same way as MTA where tricalcium silicate, calcium carbonate and zirconium oxide are mixed with water, chloride accelerator and a water-soluble polymer. Its advantages over MTA are easier handling, shorter setting time, and improved physicochemical properties.<sup>[11]</sup> However, different studies revealed a diversification in its setting time which seemed to be longer than that stated by the manufacturer (12 min).<sup>[7]</sup>

Accordingly, TheraCal LC by Bisco, a light-cured resin-modified calcium silicate-based material emerged to be used as a pulp capping material and a liner under restorative materials.<sup>[12,13]</sup> Low solubility and command set were its main merits over Biodentine. TheraCal LC paste is composed of Type III portland cement, fumed silica, strontium glass, barium sulfate ( $\text{BaSO}_4$ ), barium zirconate ( $\text{BaZrO}_3$ ), and polyethylene-glycol dimethacrylate monomers.<sup>[14]</sup> The cement is dispensed through a syringe eliminating the need for mixing

procedures. It is placed in a thickness of 1 mm to be light cured for 20 s as per the manufacturer's instructions. The polymerization of TheraCal LC is accompanied with low heat production thus reducing adverse pulpal effects when used in pulp-capping techniques.<sup>[15]</sup>

Considering the resinous nature of TheraCal LC, the hydration of the calcium silicate phase might be somehow ineffectual compared to Biodentine.<sup>[16]</sup> The actual effect of this phase on pulpal repair is thus questionable due to inadequate moisture diffusion from the pulp-dentine complex to the cement.<sup>[7,17]</sup>

Bisco has recently launched new dual cured resin-modified calcium silicate-based cement (TheraCal PT). Its primary indication is pulpotomy since it can be used in adequate thickness. It can also be utilized as a direct and an indirect pulp capping material and as a base under various substrates.

The aim of this study was to evaluate the *in vitro* bioactivity of the calcium silicate-based cements with different setting mechanisms, the newly developed TheraCal PT (dual polymerization), TheraCal LC (light polymerization) and Biodentine (chemical setting by hydration). The null hypothesis adopted is that there is no difference in bioactivity between the three cements.

## MATERIALS AND METHODS

The study is an *in vitro* research article evaluating a newly introduced dual-cured resin modified calcium silicate cement.

The products used in this study, their descriptions, setting mechanisms, compositions, manufacturers, and lot numbers are shown in Table 1.

### Specimens' preparation

Disc-shaped specimens (10 mm diameter × 2 mm thickness) were prepared using a split Teflon mold placed on a clean glass slide covered with a celluloid strip. According to the manufacturer's instruction, Biodentine was mixed after adding five drops of the liquid to the loosened powder in the capsule using an amalgamator (3M Capmix™, 3M ESPE, Germany) for 30 s with a speed of 4300 oscillations per minute. The fresh material paste was packed into the mold, covered with a celluloid strip followed by a glass slide while exerting some pressure using a C-shaped clamp to allow the extrusion of excess material according to ISO standard 9917-1:2007 for water-based cements. The

**Table 1: Products' descriptions, setting mechanisms, compositions, manufacturers and lot. numbers**

Product	Description	Setting mechanism	Composition <sup>a</sup>	Manufacturer and lot. number
Biodentine	Chemical cured tri-calcium silicate dentine substitute	Hydration	Powder: Tricalcium silicate, dicalcium silicate, calcium carbonate, oxide filler, iron oxide shade, and zirconium oxide Liquid: Water, calcium chloride and hydrosoluble polymer	Septodont, Saint-Maur-des-Fosses Cedex, France B22,105
TheraCalLC	Light cured tri-calcium silicate pulp capping material	Polymerization	Portland cement type III Polyethylene glycol dimethacrylate, barium zirconate	Bisco, Schaumburg, IL, USA 1,900,004,490
TheraCalPT	Dual cured tri-calcium silicate, pulpotomy material	Polymerization	Base: Silicate glass-mix cement, polyethylene glycol dimethacrylate, BisGMA, barium zirconate Catalyst: Barium zirconate, ytterbium fluoride, initiator	Bisco, Schaumburg, IL, USA 1,900,003,528

<sup>a</sup>Composition as stated by manufacturers in the safety data sheets. Theracal LC and Theracal PT

mix was left undisturbed in the mold for 1 h to ensure complete setting.

TheraCal LC and TheraCal PT pastes were injected directly in the mold in two successive increments of 1 mm thickness to ensure proper light curing. Each increment was light cured with an light-emitting diode light curing unit (Elipar S10, 3M ESPE, USA) with irradiance 1200 mW/cm<sup>2</sup> for 10 s. Before curing the last increment, the materials were covered with a celluloid strip and a glass slide.

Specimens were removed from the molds, immersed individually in sealed 50 mL sterile CELLSTAR<sup>®</sup> polypropylene tubes (Greiner Bio One International, GmbH, Germany) containing 5 mL deionized water (AccuGENE, Lonza) and stored in an incubator (Titanox, Italy) at 37°C. The leachates were collected from each tube on the 1<sup>st</sup>, 14<sup>th</sup>, and 28<sup>th</sup> days for Ca<sup>2+</sup> release and pH measurements. Specimens were then transferred to new tubes containing fresh deionized water.<sup>[18]</sup>

Concerning surface characterization, (environmental scanning electron microscope with energy dispersive X-ray [ESEM/EDX], Raman micro-spectroscopy, Fourier transform infrared [FTIR] spectroscopy) similar disc-shaped specimens were prepared from each cement for each characterization method. Regarding ESEM/EDX, specimens were examined immediately after setting then after 1, 14, and 28 days of storage in phosphate buffered saline (PBS). As for Raman and FTIR, specimens were analyzed immediately after setting and after 28 days of storage ( $n = 3$ ).

### *In vitro* bioactivity evaluation

#### Leachate analysis

##### *pH* evaluation

pH of the leachate was evaluated for each material after each storage period via a pH meter (B 712

LAQUA twin compact pH meter, Horiba Scientific, Japan) that was initially standardized by buffered solutions (pH 7) and recalibrated before testing each new specimen. After specimen removal and shaking the storage tube for 5 s, 1 mL from each leachate was aspirated using a micropipette (TopPette, Dragon Laboratory Instruments, China) and was placed in the pH meter measuring lens. For each sample, the pH was measured twice to calculate a mean value.

##### *Calcium release evaluation*

Ca<sup>2+</sup> release of the tested materials at the predetermined time intervals ( $n = 7$ ) was measured using inductively coupled plasma-optical emission spectrometry.<sup>[19]</sup> It was performed through Agilent 5100 Synchronous Vertical Dual View with Agilent Vapor Generation Accessory. Before analysis, the leachates were filtered and acidified using a 10% HNO<sub>3</sub> solution. HNO<sub>3</sub> with 5, 10, and 15 ppm Ca was used as a series concentration for calibration before measuring the released calcium. The amount of Ca<sup>2+</sup> was measured in ppm.

#### Surface characterization of the cement discs

##### *Environmental scanning electron microscope with energy dispersive X-ray analysis*

The surfaces of the specimens were examined without any modifications using an ESEM (TESCAN VEGA3 Czech republic) with attached EDX<sup>[20]</sup> from Bruker, immediately after setting and after 1, 14, and 28 days of storage in PBS. The discs were examined at different magnifications and elemental analysis was performed at different points on the cements' discs. After each examination, the discs were transferred to fresh 5 mL PBS and stored in the incubator till the next examination.

##### *Attenuated total reflectance/Fourier transform infrared spectroscopy*

Infrared (IR) spectra were recorded on a Vertex 70 FTIR (Bruker-Optics, Germany) equipped with

attenuated total reflectance (ATR) accessory and a deuterated triglycine sulfate detector. A resolution of 2 cm<sup>-1</sup> with a range from 4000cm<sup>-1</sup> to 600 cm<sup>-1</sup> was utilized. The diameter of ATR accessory was 2 mm diameter and the IR penetration power was about 2 μm. Spectra were accumulated for at least 10 times to avoid any fluctuations in the detection system.

### Raman spectroscopy and mapping

The surfaces of prepared samples were first imaged using a bright field microscope showing a nonhomogenized white layer. Such layer was further characterized using Raman spectroscopy. Raman single point measurements and imaging were performed using Alpha 300R/AS, Witec, Germany. High-resolution imaging was achieved through applying the smallest confocal volume. A ×100 objective lens with high numerical aperture was utilized for both single point and surface mapping. The 532 nm laser was used, its power density had been optimized to 70 mW/mm<sup>2</sup> by testing the exposed area with different laser powers using an optical microscope. The laser power was doubled in the case of mapping to reduce the exposure time at every point. The resolving grating was 600 g/mm with Blazing = 500 nm. Single point spectra were collected for 900 s for every sample. The mapped surface area was 25 by 25μ with 150 pins, and exposure time was 1 s for every pin. The band at 1040 cm<sup>-1</sup> attributed to phosphate (PO<sub>4</sub>)<sup>-3</sup> was used as a specific peak to obtain Raman mapping.

### Statistical analysis

IBM SPSS statistics data editor version 24 (IBM Corp, Armonk, New York, USA) was used. For both pH and calcium ions release test, data were checked for normality using the Kolmogorov–Smirnov test and Shapiro test, and data were found to be normally distributed. Two-way repeated measure analysis of variance test was carried out followed by Bonferroni *post hoc* test for multiple comparisons. Sample size was confirmed with statistical power analysis for each test with observed power more than 0.96. In the tables, different letters represent statistically significant differences (*P* < 0.05) in the same row (capital letters) or in the same column (lower case letters).

## RESULTS

### Leachate analysis

#### pH results

All materials showed an increasing pattern in pH

mean values till day 14 followed by an insignificant decrease on day 28, as shown in Figure 1. Biodentine leachate showed significantly higher pH values compared to those of TheraCal LC and TheraCal PT at all time intervals (*P* < 0.05). TheraCal LC leachate exhibited significantly higher pH compared to TheraCal PT on the 1<sup>st</sup> day only.

### Calcium ion release

Figure 2 illustrates Ca<sup>2+</sup> release data. Biodentine showed a descending pattern in Ca<sup>2+</sup> release with significantly lower mean values after 28 days. Despite this decreasing pattern, Bonferroni *post hoc* test showed that the mean values for Biodentine were significantly higher at all time intervals compared to TheraCal LC and PT. TheraCal LC displayed a decreasing pattern in Ca<sup>2+</sup> release for 14 days followed by a significant drop after 28 days. TheraCal PT revealed limited Ca<sup>2+</sup> release with a descending pattern throughout the 28 days. TheraCal PT showed significantly lower Ca<sup>2+</sup> release after 14 days compared to TheraCal LC.

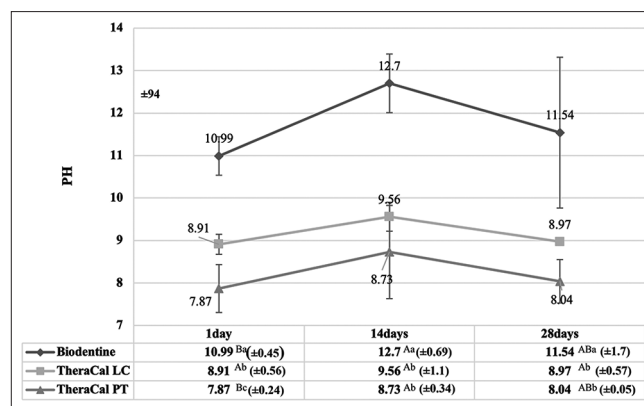


Figure 1: Line chart with table representing pH results of Biodentine, TheraCal LC, and TheraCal PT.

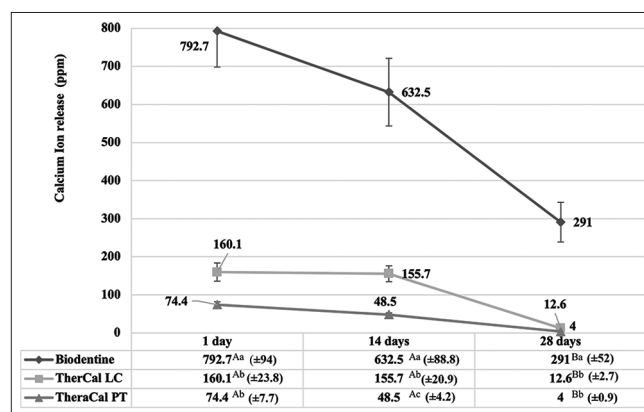


Figure 2: Line chart and table representing calcium ion release results of Biodentine, TheraCal LC, and TheraCal PT.

## Surface characterization

### *Environmental scanning electron microscope with energy dispersive X-ray results*

Figure 3 reports the ESEM data and EDX analysis of Biodentine, TheraCal LC, and TheraCal PT immediately after setting. Biodentine displayed a uniform surface containing interspersed particles with a degree of porosity. EDX analysis showed high peaks of calcium, silica, and oxygen which are the main elements of tricalcium silicate. Chlorine from the aqueous calcium chloride, limited amounts of zirconia radiopacifier, and carbon from calcium carbonate were also detected. The set TheraCal LC and TheraCal PT specimens displayed mineral particles evenly distributed in the organic resin matrix resembling that of set resin composite. The EDX spectrum showed the presence of oxygen and carbon which are the characteristic elements of the organic phase. TheraCal LC showed calcium and silicon indicating the presence of calcium silicate particles. Silica from silicate glass was present in TheraCal PT together with limited amounts of fluoride and aluminum. No calcium was detected.

ESEM data and EDX analysis of Biodentine, TheraCal LC, and TheraCal PT after 1-day storage are shown in Figure 4. Biodentine surface showed a degree of densification since porosities were filled with hydration products, calcium silicate hydrate, and calcium hydroxide. Few spherical precipitates were also detected on the surface. EDX analysis detected the presence of calcium, silicon, oxygen, and traces of phosphorous. TheraCal LC displayed few spherical precipitates on the surface. Calcium, silicon, carbon, and oxygen in addition to traces of phosphorous were detected. TheraCal PT showed no precipitates where carbon and oxygen were present as major components for resin matrix. Small traces of calcium, fluoride, and aluminum were detected.

Following 14 days storage of Biodentine, TheraCal LC, and TheraCal PT, globular deposits were detected covering the majority of Biodentine surface [Figure 5]. Calcium was detected and the level of phosphate increased considerably. TheraCal LC also showed an evident globular surface layer coating most of the specimen's surface as shown in Figure 5. EDX analysis revealed the presence of calcium, phosphate, and oxygen which might indicate apatite formation. TheraCal PT showed limited scattered spherical precipitates on the surface.

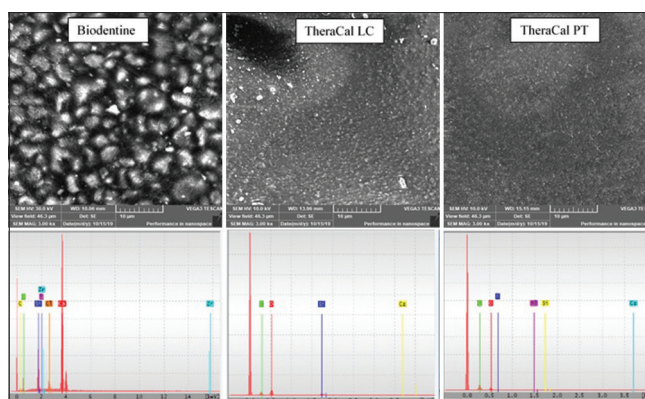


**Figure 3:** Environmental scanning electron microscope images with corresponding energy dispersive X-ray analysis for Biodentine, TheraCal LC, and TheraCal PT immediately after setting.

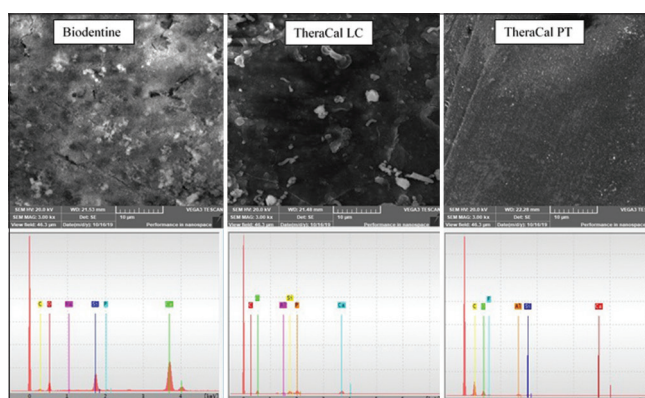


**Figure 4:** Environmental scanning electron microscope images with corresponding energy dispersive X-ray analysis for Biodentine, TheraCal LC, and TheraCal PT after 1 day immersion in phosphate-buffered saline.

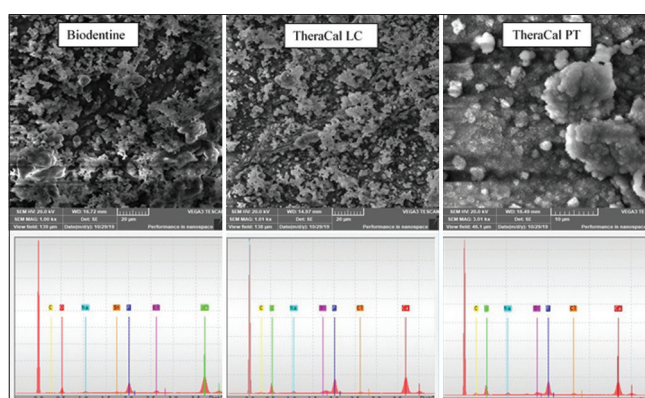


**Figure 5:** Environmental scanning electron microscope images with corresponding energy dispersive X-ray analysis for Biodentine, TheraCal LC and TheraCal PT after 14 days immersion in phosphate-buffered saline.

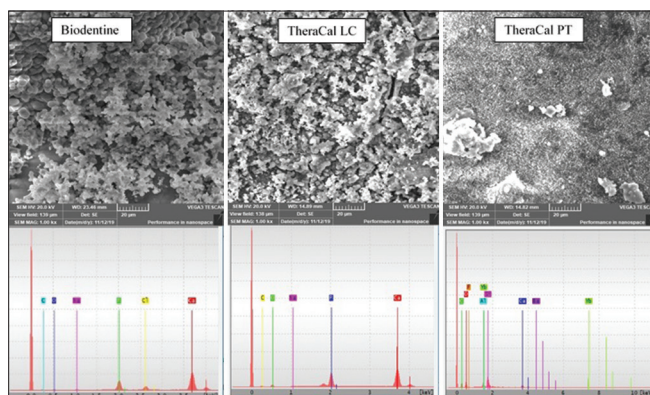
Carbon and oxygen were present as major elements of the resin matrix with limited amounts of calcium and phosphorous.

Figure 6 shows ESEM data and EDX analysis of Biodentine, TheraCal LC, and TheraCal PT after 28 days. Both Biodentine and TheraCal LC showed a continuous layer of globular particles covering the entire surface of the specimen. Such layer is formed mainly of calcium, phosphate, and oxygen that might indicate apatite layer development. No silicon could be detected as the precipitated layer completely covered the discs' surfaces. TheraCal PT showed the presence of few precipitates on the surface. EDX analysis revealed the presence of oxygen and carbon as major constituents together with calcium and silicon.

#### Attenuated total reflectance/Fourier transform infrared analysis

Figure 7 reports overlaid IR spectra for each of Biodentine [Figure 7a], TheraCal PT [Figure 7b] and TheraCal LC [Figure 7c] both before immersion (control) and after 28 days of immersion in PBS.

Fresh Biodentine samples presented bands attributed to O-Si-O ( $813\text{ cm}^{-1}$ ), and O-Si-O/Si-O-Si ( $524\text{ cm}^{-1}$ ,  $455\text{ cm}^{-1}$ ). Silica group was also detected at  $640\text{ cm}^{-1}$  in addition to a silanol group that might be part of the calcium silicate hydrate layer (CSH) at  $956\text{ cm}^{-1}$ .<sup>[21-24]</sup>



**Figure 6:** Environmental scanning electron microscope images with corresponding energy dispersive X-ray analysis for Biodentine, TheraCal LC, and TheraCal PT after 28 days immersion in phosphate-buffered saline.

The carbonate group of calcite appeared at  $875\text{ cm}^{-1}$  and about  $1458\text{ cm}^{-1}$ .<sup>[25]</sup> A band at  $3,465\text{ cm}^{-1}$  indicated the presence of  $\text{Ca}(\text{OH})_2$ . A peak representing an aliphatic C = C ( $1638\text{ cm}^{-1}$ ) may be due to the presence of the hydrosoluble polymer present in the Biodentine liquid as a water-reducing agent.<sup>[22]</sup>

After storage, the peak intensity of  $\text{Ca}(\text{OH})_2$  at  $3,465\text{ cm}^{-1}$  decreased indicating the dissolution of  $\text{Ca}(\text{OH})_2$  in PBS. Another peak for  $\text{Ca}(\text{OH})_2$  also appeared at  $1428\text{ cm}^{-1}$ .<sup>[22]</sup>

The band assigned to calcium carbonate at  $1458\text{ cm}^{-1}$  showed a reduction in peak intensity.  $\text{PO}_4^{3-}$  groups formed bands at  $560\text{ cm}^{-1}$  and  $600\text{ cm}^{-1}$  in addition to a strong band at  $1042\text{ cm}^{-1}$ .<sup>[26-28]</sup>

Analyzing freshly set TheraCal LC and TheraCal PT, the presence of silicate was noticeable at  $813\text{ cm}^{-1}$  and at  $950\text{ cm}^{-1}$  for TheraCal LC, and  $460\text{ cm}^{-1}$  for both types of cements. A very strong and broad band of silicate was also observed at  $1107\text{ cm}^{-1}$  for TheraCal LC and for TheraCal PT at  $1120\text{ cm}^{-1}$ .<sup>[22]</sup> Stretching vibration of C = O and C = C appeared at  $1720\text{ cm}^{-1}/1725\text{ cm}^{-1}$  and  $1638\text{ cm}^{-1}/1640\text{ cm}^{-1}$ , respectively, in TheraCal LC and PT spectra attributing to their polymeric content. Bands at  $1511\text{ cm}^{-1}/1513\text{ cm}^{-1}$  (C-H aromatic ring),  $1250\text{ cm}^{-1}$  (C-O),  $1300\text{ cm}^{-1}$  (C-H), and  $1385\text{ cm}^{-1}$  ( $\text{CH}_3$ ) also indicate the presence of resin.

After 28 days of storage in PBS,  $\text{PO}_4^{3-}$  groups formed bands at  $560\text{ cm}^{-1}$ ,  $600\text{ cm}^{-1}$  and  $1100\text{ cm}^{-1}$ .

The band at  $3465\text{ cm}^{-1}$  assigned to the hydroxyl groups of  $\text{Ca}(\text{OH})_2$  appeared in both types of TheraCal after storage indicating the commencement of the hydration reaction.<sup>[22]</sup>

#### Micro-Raman analysis

##### Raman spectroscopy

Raman spectra for Biodentine, TheraCal LC, and TheraCal PT both before immersion [Figure 8a] and

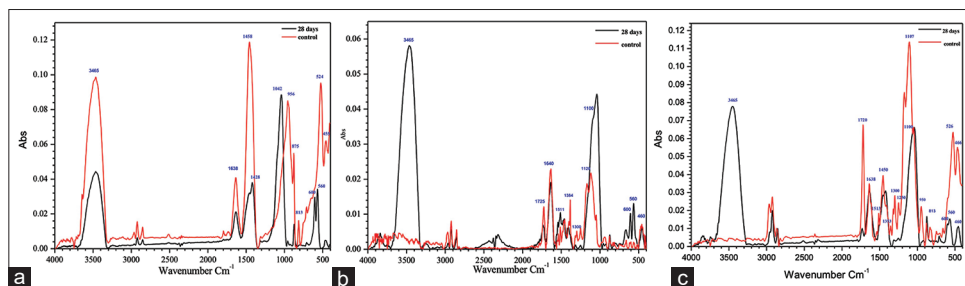


**Figure 7:** The overlaid Fourier transform infrared spectra of control samples before immersion and after 28 days for Biodentine (a), TheraCal PT (b), and TheraCal LC (c).

after 28 days of immersion in PBS [Figure 8b] are shown in figure.<sup>[8]</sup>

For freshly prepared specimens, Figure 8a indicates the presence of a band at  $1085\text{ cm}^{-1}$  assigned to Ca silicate<sup>[29]</sup> which is of better intensity in Biodentine compared to TheraCal LC, while for TheraCal PT, this band appears rare and weak. The  $\text{CaCO}_3$  band at  $1080\text{ cm}^{-1}$  was observed in Biodentine only.<sup>[30]</sup>  $\text{Ca(OH)}_2$  at  $252\text{ cm}^{-1}$  and  $356\text{ cm}^{-1}$  exhibited a medium band in Biodentine.<sup>[31]</sup> A  $\text{C}=\text{C}$  band appeared at  $1609\text{ cm}^{-1}$  assigned to the organic content of both TheraCal types.<sup>[32]</sup>

After 28 days of immersion in PBS, the recorded spectra showed additional bands at  $960\text{ cm}^{-1}$  and  $1040\text{ cm}^{-1}$  assigned to  $(\text{PO}_4)^{-3}$ .<sup>[33]</sup> It is noteworthy that the  $(\text{PO}_4)^{-3}$  band at  $1040\text{ cm}^{-1}$  appeared in all cement types while that at  $960\text{ cm}^{-1}$  appeared in Biodentine and TheraCal LC only.  $\text{Ca(OH)}_2$  bands at  $252\text{ cm}^{-1}$  and  $356\text{ cm}^{-1}$  appeared in TheraCal LC and TheraCal PT after immersion in PBS.

#### Raman mapping

Figure 9 shows the Raman mapping for Biodentine [Figure 9a], TheraCal LC [Figure 9b], and TheraCal PT [Figure 9c] at symmetric Raman band  $1040\text{ cm}^{-1}$  attributed to phosphate  $(\text{PO}_4)^{-3}$  both before immersion (control) and after 28 days of immersion. Regarding the nonimmersed samples, charge-coupled device (CCD) counts showed peaks of 2.8 maximum, indicating nearly no presence of phosphate. Most probably such color-coded peaks were due to noise during Raman analysis.

After immersion, Biodentine image showed major peaks in the cyan, green, and blue regions indicating about 9–15 CCD counts. The maximum concentration of the phosphate bond might reach 27 CCD counts represented by few yellow peaks. As for TheraCal LC, most of the peaks were in the cyan, blue, and green regions referring to ~5–6 CCD counts. A few distributed yellow peaks were present indicating ~15 CCD counts.

The maximum phosphate bond concentration for TheraCal PT stored samples was 9–10 CCD counts (yellow and orange peaks). Major peak intensities were within the blue and green region representing approximately 5–6 CCD counts. Phosphate concentration dispersed over the investigated areas thus seemed to be of lower CCD counts compared to Biodentine and TheraCal LC.

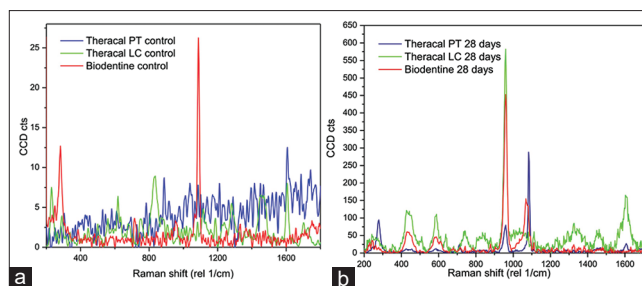


**Figure 8:** The overlaid Raman spectra of Biodentine, TheraCal LC and TheraCal PT before immersion (a) and after 28 days (b).

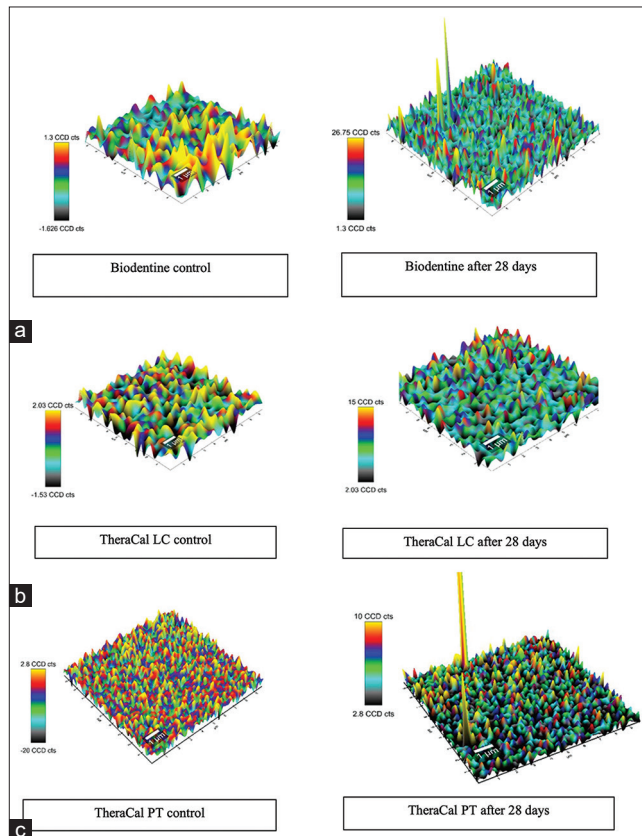


**Figure 9:** The Raman mapping of Biodentine (a), TheraCal LC (b), and TheraCal PT (c) for control samples and after 28 days immersion presenting the distribution of  $(\text{PO}_4)^{-3}$  at  $1040\text{ cm}^{-1}$ .

## DISCUSSION

HCSCs have shown the capability of creating a satisfactory “bioactive” surface possessing a suitable architecture following immersion in various simulated body fluids. Such surface was established through calcium phosphates nucleation and the development of an apatite layer. HCSCs are a subject of numerous improvements and modifications.<sup>[1,34]</sup> They exhibit variations in their setting modes including hydration reactions, light, and dual polymerization reactions. However, limited researches are present regarding

some of these cements.<sup>[35]</sup> To the best of our knowledge, a single study was recently published regarding TheraCal PT bioactivity.<sup>[36]</sup> This study, thus, sought to investigate the bioactivity of dual-cured TheraCal PT as compared to light-cured TheraCal LC and Angelus MTA.

Ca<sup>2+</sup> release together with alkalizing activity is the foundation for favorable biological properties of HCSC utilized in pulp therapy and regenerative endodontic procedures.<sup>[19,37]</sup> The leached Ca<sup>2+</sup> enhances the growth of human dental pulp cells in a dose-dependent manner and boosts the activity of pyrophosphatase, which aids in maintaining dentine mineralization and the development of a dentine bridge.<sup>[20,38]</sup> Furthermore, the production of hydroxyl ions increases the pH of the surrounding environment causing pulpal tissue irritation. Superficial necrosis thus develops on exposed pulp, stimulating mineralization against the necrotic zone. Hydroxyl ions also encourage the production of alkaline phosphatase and bone morphogenic proteins, which take part in the mineralization process.<sup>[37]</sup> Accordingly, it was of prime importance to evaluate Ca<sup>2+</sup> release and assess the pH of the leachates of different cements.

PBS was used in various researches mimicking the physiologic body fluids for evaluation of the *in vitro* bioactivity of Biodentine, TheraCal and MTA like materials. Consequently, PBS was selected as an immersion medium in this study.<sup>[18]</sup>

Biodentine exhibited the highest levels of Ca<sup>2+</sup> release throughout all time intervals while both TheraCal PT and LC showed less Ca<sup>2+</sup> release with no significant difference between them. These findings are consistent with those of previous studies stating that resin modified HCSCs showed limited bioactivity and reduced Ca<sup>2+</sup> release compared to Biodentine.<sup>[16,19,20,39,40]</sup>

Compositional differences between Biodentine and TheraCal LC might be a plausible explanation for such Ca<sup>2+</sup> release results. Biodentine powder is formed mainly of tricalcium silicate (80.1%) while its liquid contains a calcium chloride accelerator that functions as a water-reducing agent. Sources of calcium thus seem to be abundant in Biodentine composition.<sup>[16,41]</sup>

Contrarily, TheraCal LC's safety datasheet stated that it comprises a resin matrix (10%–30%) formed mainly of polyethylene glycol dimethacrylate while portland cement Type III which acts as a calcium ion

source constitutes a percentage that does not exceed 50% of the total composition. Such configuration indicates less Ca<sup>2+</sup> sources in TheraCal LC compared to Biodentine. Similarly, the aforementioned explanation can be applied to TheraCal PT since it is a resin-modified calcium silicate cement consisting of polyethylene glycol dimethacrylate (10%–30%) and Bis-GMA (5%–10%) resin matrix as per its safety datasheet. It is noteworthy that the safety data sheet of TheraCal PT (base and catalyst) did not mention the presence of calcium by any means in its composition.

Another reason for higher Ca<sup>2+</sup> release of Biodentine is its porous [Figure 3] extremely hydrophilic structure in which hydration occurs significantly producing large amounts of calcium silicate hydrate and calcium hydroxide.<sup>[16,40]</sup>

On the contrary, the resinous structure of TheraCal LC and TheraCal PT lacks sufficient porosities to allow such hydration reaction to occur. They rely mainly on water sorption and diffusion within the hydrophobic resin matrix which is somehow limited. It could be postulated that deficient hydration reactions of TheraCal LC and TheraCal PT is due to the sparse moisture diffusion in the set resin material causing deficient Ca<sup>2+</sup> release.<sup>[16,42]</sup> Biodentine showed a significant drop in Ca<sup>2+</sup> release at day 28; a similar pattern was detected in a previous study.<sup>[43]</sup>

Concerning alkalizing activity, Biodentine showed significantly higher alkalizing potential at all time intervals compared to both TheraCal PT and TheraCal LC and this goes in line with other similar studies.<sup>[21,33]</sup> TheraCal LC alkalizing activity was significantly higher than that of TheraCal PT after 1 day; however, no difference was detected after 14 and 28 days.

Alkalizing potential of calcium silicate cements is due to the formation of calcium hydroxide that undergoes ionization when subjected to moisture producing hydroxyl ions.<sup>[3]</sup> Accordingly, an increase in Ca<sup>2+</sup> release is suggestive of higher hydroxyl ion diffusion. Low solubility of TheraCal LC together with limited water sorption of its resin matrix hinders the hydration reaction of calcium silicate to calcium hydroxide; hence reducing its alkalizing activity.<sup>[14]</sup> Owing to its resinous nature, such postulations appear applicable as well to TheraCal PT's results.

pH results were further supported by ATR/FTIR analysis, where Ca (OH)<sub>2</sub> was detected in Biodentine both before and after immersion in PBS at 1428 cm<sup>-1</sup> and 3,465 cm<sup>-1</sup> and in both types of TheraCal at

3465  $\text{cm}^{-1}$  only after storage. Raman analysis followed nearly the same trend where  $\text{Ca}(\text{OH})_2$  bands for both types of TheraCal appeared only after storage indicating less sources of hydroxyl ions in TheraCal.

All silicate cements showed a significantly increasing pattern in pH up till 14 days. Such increase in pH values with time has been observed previously.<sup>[44]</sup>

Calcium silicate-based cements are capable of developing hydroxyapatite precipitates when placed in contact with phosphate-containing physiological fluids.<sup>[45]</sup> This formed apatite coating enhances cell attachment, differentiation, and tissue repair associated with mineralized tissue synthesis.<sup>[46]</sup> Surface characterization of discs soaked in PBS solution at different time intervals was thus performed in the current study using ESEM/EDX analysis, Raman spectroscopy, and FTIR spectroscopy.

ESEM was used instead of the conventional SEM to avoid any surface preparation or coating of the discs before imaging. This prevented any change in their surface chemistry and allowed evaluation of the same disc at different time intervals as intended.<sup>[47]</sup> Raman and IR spectroscopy are corresponding techniques capable of detecting silicate, carbonate, hydroxyl and phosphate vibrational modes, representing the hydration process of the cement along with apatite formation.

ESEM of freshly set Biodentine showed a uniform surface containing interspersed particles. EDX displayed the presence of calcium (approximately 50%) from tricalcium silicate. Regarding TheraCal LC, EDX analysis at various points showed traces of calcium (1wt%), while in TheraCal PT no calcium was detected at any points of analysis [Figure 3]. Such findings are in line with calcium release results, where Biodentine showed the significantly highest values due to its higher calcium content. FTIR and Raman spectroscopy for freshly prepared specimens seemed to support EDX analysis where calcium hydroxide and calcium carbonate bands as  $\text{Ca}^{2+}$  sources were present in Biodentine but absent in both types of TheraCal [Figures 7 and 8]. Calcium silicate bands were common in Biodentine, TheraCal LC, and TheraCal PT, however for TheraCal PT, these bands were the fewest (460  $\text{cm}^{-1}$ , 1120  $\text{cm}^{-1}$ ) in FTIR analysis and of very weak intensity in Raman analysis.

Storage of Biodentine and TheraCal LC discs for 14 and 28 days in PBS led to the formation of continuous

layers of globular deposits on their surfaces. EDX analysis at various points of these layers revealed the presence of both calcium and phosphate with increased peak intensities [Figures 5 and 6] which might enhance the formation of an appetite layer.<sup>[48]</sup> However, TheraCal PT discs exhibited scarce precipitates on their surface with low calcium and phosphate percentages as detected by EDX. Such EDX analysis pattern was in line with that of Rodríguez-Lozano *et al.*<sup>[36]</sup>

Such findings were further confirmed via FTIR and Raman spectroscopy. FTIR spectra for stored Biodentine, TheraCal LC, and TheraCal PT showed bands corresponding to  $\text{PO}_4^{3-}$  which are attributable to the presence of hydroxyapatite [Figure 7].<sup>[26,27]</sup>

Moreover, peak heights of the phosphate bands in TheraCal PT at 560, 600, and 1100  $\text{cm}^{-1}$  were approximately one third that of Biodentine and TheraCal LC [Figure 7]. As for Raman spectroscopy, bands at 960 and 1040  $\text{cm}^{-1}$  assigned to  $(\text{PO}_4)^{3-}$  were detected. TheraCal PT exhibited the weakest band intensity relative to Biodentine and TheraCal LC, thus failed to develop appropriate phosphate deposits on its surface [Figure 8]. It is worth noting that Theracal PT was not able to form  $(\text{PO}_4)^{3-}$  bands at 960  $\text{cm}^{-1}$  as Theracal LC and Biodentine did [Figure 8].

Raman mapping results at 1040  $\text{cm}^{-1}$  were also in line with that of the other surface characterization methods where Biodentine samples exhibited the highest concentration of  $(\text{PO}_4)^{3-}$  bonds followed by TheraCal LC while Theracal PT showed the weakest peak intensities for  $(\text{PO}_4)^{3-}$  bonds with the least CCD counts distribution [Figure 9].

Although TheraCal LC showed reduced  $\text{Ca}^{2+}$  release compared to Biodentine, it was able to form surface deposits rich in calcium and phosphate as those of Biodentine. Limited moisture diffusion within the resin matrix of TheraCal LC<sup>[16]</sup> might have hindered its hydration reaction and  $\text{Ca}^{2+}$  release; however, it was sufficient to develop calcium and phosphate deposits on its surface.

Combined results of  $\text{Ca}^{2+}$  release and alkalinizing potential pointed out the high bioactivity of Biodentine compared to TheraCal LC. However, TheraCal LC still developed a mineralized layer rich in calcium and phosphate despite its lower  $\text{Ca}^{2+}$  release. As for TheraCal PT, its limited  $\text{Ca}^{2+}$  release, low alkalinizing potential as well as failure to develop adequate calcium phosphate deposits reflected its poor *in vitro*

bioactivity. Based on the above findings, the null hypothesis was thus rejected.

One of the limitations of this study is the lack of clinical simulation, thus bioactivity results might appear higher than expected in clinical situation where availability of moisture is limited. However, evaluation of hydration and bioactivity of calcium silicate – based cements is usually performed *in vitro* in standardized conditions to allow data correlation.<sup>[40]</sup> Moreover, the novelty of TheraCal PT favors conducting the study initially outside the biological context to be able to compare it with other HCSCs. Another drawback is the absence of enough previous studies in the literature concerning TheraCal PT to confirm or reject our findings.

## CONCLUSION

Within the limitations of this study, it could be deduced that TheraCal PT possesses reduced *in vitro* bioactivity in terms of Ca<sup>2+</sup> release, alkalizing potential and apatite formation compared to Biodentine and TheraCal LC. Biodentine exhibits potent *in vitro* bioactivity compared to TheraCal LC which shows potential bioactivity in the form of precipitate formation. Further laboratory investigations and clinical trials regarding bioactivity of these materials are still required.

## Acknowledgment

The authors would like to thank Alex Dent Company, the official distributor of Bisco Inc. in Egypt for supplying the required materials from Bisco for free.

## Financial support and sponsorship

Nil.

## Conflicts of interest

The authors of this manuscript declare that they have no conflicts of interest, real or perceived, financial or nonfinancial in this article.

## REFERENCES

- Prati C, Gandolfi MG. Calcium silicate bioactive cements: Biological perspectives and clinical applications. *Dent Mater* 2015;31:351-70.
- Parirokh M, Torabinejad M, Dummer PMH. Mineral trioxide aggregate and other bioactive endodontic cements: an updated overview – Part I: Vital pulp therapy. *Int Endod J* 2018;51:177-205.
- Camilleri J. Mineral trioxide aggregate: Present and future developments. *Endod Top* 2015;32:31-46.
- Wang X, Chang J, Hu S. A study on the sealing ability and antibacterial activity of Ca<sub>3</sub>SiO<sub>5</sub>/CaCl<sub>2</sub> composite cement for dental applications. *Dent Mater J* 2012;31:617-22.
- Peskersoy C, Lukarcanin J, Turkun M. Efficacy of different calcium silicate materials as pulp-capping agents: Randomized clinical trial. *J Dent Sci* 2021;16:723-31.
- Cervino G, Laino L, D'Amico C, Russo D, Nucci L, Amoroso G, *et al.* Mineral trioxide aggregate applications in endodontics: A review. *Eur J Dent* 2020;14:683-91.
- Dawood AE, Parashos P, Wong RH, Reynolds EC, Manton DJ. Calcium silicate-based cements: Composition, properties, and clinical applications. *J Investig Clin Dent* 2017;8:e12195.
- Camilleri J, Sorrentino F, Damidot D. Investigation of the hydration and bioactivity of radiopacified tricalcium silicate cement, Biodentine and MTA Angelus. *Dent Mater* 2013;29:580-93.
- Wongkornchaowalit N, Lertchirakarn V. Setting time and flowability of accelerated Portland cement mixed with polycarboxylate superplasticizer. *J Endod* 2011;37:387-9.
- Domingos Pires M, Cordeiro J, Vasconcelos I, Alves M, Quaresma SA, Ginjeira A, *et al.* Effect of different manipulations on the physical, chemical and microstructural characteristics of Biodentine. *Dent Mater* 2021;37:e399-406.
- Saghiri MA, Orangi J, Asatourian A, Gutmann JL, Garcia-Godoy F, Lotfi M, *et al.* Calcium silicate-based cements and functional impacts of various constituents. *Dent Mater J* 2017;36:8-18.
- Karadas M, Cantekin K, Gumus H, Ateş SM, Duymuş ZY. Evaluation of the bond strength of different adhesive agents to a resin-modified calcium silicate material (TheraCal LC). *Scanning* 2016;38:403-11.
- Gasperi TL, Silveira JA, Schmidt TF, Teixeira CD, Garcia LD, Bortoluzzi EA. Physical-mechanical properties of a resin-modified calcium silicate material for pulp capping. *Braz Dent J* 2020;31:252-6.
- Gandolfi MG, Siboni F, Prati C. Chemical–physical properties of TheraCal, a novel light-curable MTA-like material for pulp capping. *Int Endod J* 2012;45:571-9.
- Savas S, Botsali MS, Kucukyilmaz E, Sari T. Evaluation of temperature changes in the pulp chamber during polymerization of light-cured pulp-capping materials by using a VALO LED light curing unit at different curing distances. *Dent Mater J* 2014;33:764-9.
- Camilleri J. Hydration characteristics of Biodentine and Theracal used as pulp capping materials. *Dent Mater* 2014;30:709-15.
- Sahin N, Saygili S, Akcay M. Clinical, radiographic, and histological evaluation of three different pulp-capping materials in indirect pulp treatment of primary teeth: A randomized clinical trial. *Clin Oral Investig* 2021;25:3945-55.
- Di Foggia M, Prati C, Gandolfi MG, Taddei P. Spectroscopic and morphological data assessing the apatite forming ability of calcium hydroxide-releasing materials for pulp capping. *Data Brief* 2019;23:103719.
- Koutroulis A, Kuehne SA, Cooper PR, Camilleri J. The role of calcium ion release on biocompatibility and antimicrobial properties of hydraulic cements. *Sci Rep* 2019;9:19019.
- Gandolfi MG, Siboni F, Botero T, Bossù M, Riccitiello F,

- Prati C. Calcium silicate and calcium hydroxide materials for pulp capping: biointeractivity, porosity, solubility and bioactivity of current formulations. *J Appl Biomater Funct Mater* 2015;13:43-60.
21. Solanki NP, Venkappa KK, Shah NC. Biocompatibility and sealing ability of mineral trioxide aggregate and biodentine as root-end filling material: A systematic review. *J Conserv Dent* 2018;21:10-5.
  22. Yu P, Kirkpatrick RJ, Poe B, McMillan PF, Cong X. Structure of calcium silicate hydrate (C-S-H): Near-, Mid-, and Far-infrared spectroscopy. *J Am Ceram Soc* 1999;82:742-8.
  23. Girsova MA, Golovina GF, Kurilenko LN, Anfimova IN. Infrared spectroscopy of bismuth-containing composites based on porous high-silica glass. *Glas Phys Chem* 2020;46:138-45.
  24. Rubio F, Rubio J, Oteo JL. A FT-IR study of the hydrolysis of tetraethylorthosilicate (TEOS). *Spectrosc Lett* 1998;31:199-219.
  25. Gunasekaran S, Anbalagan G, Pandi S. Raman and infrared spectra of carbonates of calcite structure. *J Raman Spectrosc* 2006;37:892-9.
  26. Gheisari H, Karamian E, Abdollahi M. A novel hydroxyapatite-hardystonite nanocomposite ceramic. *Ceram Int* 2015;41:5967-75.
  27. Gandolfi MG, Taddei P, Tinti A, Prati C. Apatite-forming ability (bioactivity) of ProRoot MTA. *Int Endod J* 2010;43:917-29.
  28. Abifarink JK, Obada DO, Dauda ET, Dodoo-Arhin D. Experimental data on the characterization of hydroxyapatite synthesized from biowastes. *Data Brief* 2019;26:104485.
  29. Gasharova B, Garbev K, Bornefeld M, Black L, Stemmermann P. Raman and IR spectroscopic study of nano-crystalline calcium silicate hydrates of type CSH (I). *Acta Cryst* 2006;62:s208.
  30. De La Pierre M, Carteret C, Maschio L, André E, Orlando R, Dovesi R. The Raman spectrum of CaCO<sub>3</sub> polymorphs calcite and aragonite: A combined experimental and computational study. *J Chem Phys* 2014;140:164509.
  31. Pisu FA, Chiriu D, Ricci PC, Carbonaro CM. Defect related emission in calcium hydroxide: The controversial band at 780 cm<sup>-1</sup>. *Crystals* 2020;10:266.
  32. Zou Y, Armstrong SR, Jessop JL. Quantitative analysis of adhesive resin in the hybrid layer using Raman spectroscopy. *J Biomed Mater Res A* 2010;94:288-97.
  33. Nosenko VV, Yaremko AM, Dzhagan VM, Vorona IP, Romanyuk YA, Zatovsky IV. Nature of some features in Raman spectra of hydroxyapatite-containing materials. *J Raman Spectrosc* 2016;47:726-30.
  34. Ha W, Kahler B, Walsh LJ. Classification and nomenclature of commercial hygroscopic dental cements. *Eur Endod J* 2017;2:1-10.
  35. Kunert M, Lukomska-Szymanska M. Bio-inductive materials in direct and indirect pulp capping-a review article. *Materials (Basel)* 2020;13:1204.
  36. Rodríguez-Lozano FJ, López-García S, García-Bernal D, Sanz JL, Lozano A, Pecci-Lloret MP, *et al.* Cytocompatibility and bioactive properties of the new dual-curing resin-modified calcium silicate-based material for vital pulp therapy. *Clin Oral Investig* 2021;25:5009-24.
  37. Kurun Aksoy M, Tuğla Oz F, Orhan K. Evaluation of calcium (Ca<sup>2+</sup>) and hydroxide (OH<sup>-</sup>) ion diffusion rates of indirect pulp capping materials. *Int J Artif Organs* 2017;40:641-6.
  38. Bortoluzzi EA, Niu LN, Palani CD, El-Awady AR, Hammond BD, Pei DD, *et al.* Cytotoxicity and osteogenic potential of silicate calcium cements as potential protective materials for pulpal revascularization. *Dent Mater* 2015;31:1510-22.
  39. Pedano MS, Li X, Yoshihara K, Landuyt KV, Van Meerbeek B. Cytotoxicity and bioactivity of dental pulp-capping agents towards human tooth-pulp cells: A systematic review of *in-vitro* studies and meta-analysis of randomized and controlled clinical trials. *Materials (Basel)* 2020;13:2670.
  40. Camilleri J, Laurent P, About I. Hydration of Biodentine, Theracal LC, and a prototype tricalcium silicate-based dentin replacement material after pulp capping in entire tooth cultures. *J Endod* 2014;40:1846-54.
  41. Kaur M, Singh H, Dhillon JS, Batra M, Saini M. MTA versus biodentine: Review of literature with a comparative analysis. *J Clin Diagn Res* 2017;11:G01-5.
  42. Arandi NZ, Rabi T. TheraCal LC: From biochemical and bioactive properties to clinical applications. *Int J Dent* 2018;2018:3484653.
  43. Rajasekharan S, Martens LC, Cauwels R, Anthonappa RP. Biodentine™ material characteristics and clinical applications: A 3 year literature review and update. *Eur Arch Paediatr Dent* 2018;19:1-22.
  44. Chen CC, Ho CC, David Chen CH, Ding SJ. Physicochemical properties of calcium silicate cements for endodontic treatment. *J Endod* 2009;35:1288-91.
  45. Han L, Okiji T. Bioactivity evaluation of three calcium silicate-based endodontic materials. *Int Endod J* 2013;46:808-14.
  46. Yamamoto S, Han L, Noiri Y, Okiji T. Evaluation of the Ca ion release, pH and surface apatite formation of a prototype tricalcium silicate cement. *Int Endod J* 2017;50 Suppl 2:e73-82.
  47. Gandolfi MG, Siboni F, Polimeni A, Bossù M, Riccitiello F, Rengo S, *et al.* *In vitro* screening of the apatite-forming ability, biointeractivity and physical properties of a tricalcium silicate material for endodontics and restorative dentistry. *Dent J* 2013;1:41-60.
  48. Corral Nuñez C, Covarrubias C, Fernandez E, Oliveira OB. Enhanced bioactive properties of Biodentine™ modified with bioactive glass nanoparticles. *J Appl Oral Sci* 2017;25:177-85.